EUROPHYSICS LETTERS 15 March 2006

Europhys. Lett., **73** (6), pp. 851–857 (2006)
DOI: 10.1209/epl/i2005-10486-2

Response maxima in time-modulated turbulence: Direct numerical simulations

A. K. Kuczaj[1](*), B. J. Geurts[1,2] and D. Lohse[3](**)

[1] *Department of Applied Mathematics and J. M. Burgers Center for Fluid Dynamics University of Twente - P.O. Box 217, 7500 AE Enschede, The Netherlands*
[2] *Department of Applied Physics, Eindhoven University of Technology P.O. Box 513, 5300 MB Eindhoven, The Netherlands*
[3] *Department of Applied Physics and J. M. Burgers Center for Fluid Dynamics University of Twente - P.O. Box 217, 7500 AE Enschede, The Netherlands*

received 24 September 2005; accepted in final form 30 January 2006
published online 15 February 2006

PACS. 47.27.Rc – Turbulence control.
PACS. 47.27.E- – Turbulence simulation and modeling.
PACS. 47.27.Gs – Isotropic turbulence; homogeneous turbulence.

Abstract. – The response of turbulent flow to time-modulated forcing is studied by direct numerical simulations of the Navier-Stokes equations. The large-scale forcing is modulated via periodic energy input variations at frequency ω. The response is maximal for frequencies in the range of the inverse of the large eddy turnover time, confirming the mean-field predictions of von der Heydt, Grossmann and Lohse (*Phys. Rev. E*, **67** (2003) 046308). In accordance with the theory the response maximum shows only a small dependence on the Reynolds number. At sufficiently high frequencies the amplitude of the kinetic energy response decreases as $1/\omega$. For frequencies beyond the range of maximal response, a significant change in the phase-shift relative to the time-modulated forcing is observed. For large ω the phase shift approaches roughly 90° for the total energy and 180° for the energy dissipation rate.

Introduction. – Recently, response maxima in time-modulated turbulence have been predicted within a mean-field theory of turbulence [1]. Subsequently, such response maxima were found [2] in numerical simulations of simplified dynamical turbulence models such as the GOY model [3–5] or the reduced wave vector approximation (REWA) [6,7]. However, these response maxima computed in [2] were not pronounced at all, due to the approximate treatment of the small scales in either of these approaches. Indications of response maxima resulting from time-modulated forcing have subsequently also been seen in experiment [8]. The experimental observations were done by introducing a time-dependent swirl to fluid in a closed container and monitoring the energy injection rate. The selected set-up did not allow to identify possible flow-structuring under resonance conditions, nor to conclusively distinguish such resonance phenomena from flow-organization associated with the size of the container. Earlier, response functions of jet turbulence and thermally driven turbulence were measured [9]. The response of various space-dependent quantities in turbulent channel flow to periodically forced oscillations was examined in ref. [10]. There the boundary layers and thus the anisotropy of the flow play a major role, but go beyond the scope of presented work; their role is a possible direction of further numerical investigations.

(*) E-mail: a.k.kuczaj@utwente.nl
(**) E-mail: d.lohse@utwente.nl

The purpose of this paper is to complement these theoretical, numerical, and experimental observations by direct numerical simulations (DNS) of turbulence, subject to time-modulated large-scale forcing. In a turbulent flow whose large-scale forcing is periodically modulated in time, all typical flow-properties develop a complex time dependence. However, averaging such turbulent time dependence, conditioned on the phase of the periodic modulation, yields a clear and much simpler periodic pattern [2]. The dependence of the conditionally averaged response on the frequency of the modulation may be quantified by monitoring changes in flow properties such as total energy, dissipation rate, or Taylor-Reynolds number. In case of a fast modulation with a frequency $\omega \gg \omega_L$, where ω_L is the inverse large eddy turnover time, only a modest effect on the flow is expected, or none at all. Likewise, if $\omega \ll \omega_L$ the modulation is quasi-stationary and the flow may be expected to closely resemble the corresponding unmodulated case. In between these extremes a more pronounced response may develop, which is the subject of this investigation.

The DNS approach allows to investigate in detail the response of turbulent-flow properties to periodic modulation of the forcing. In particular, we present a parameter study involving a large range of modulation frequencies for two different Reynolds numbers, and establish response maxima in a variety of flow properties. The response is found to be significantly increased at modulation frequencies on the order of the inverse of the eddy turnover time. Near resonance, the "activity" of the turbulent flow is found to be considerably higher than in the unmodulated case. At high frequencies ω the amplitude of the modulation-specific response of the kinetic energy is found to uniformly decrease to zero as ω^{-1}. This type of external control of turbulence may offer new opportunities with relevance to technological applications, *e.g.*, increased mixing efficiency.

First, the computational flow-model is introduced. Subsequently, an overview of the ensemble averaging procedure and data extraction is given. Then the main result, the response of various flow properties to time-modulated forcing, is presented.

Computational flow model. – The full Navier-Stokes equations for incompressible flow are numerically solved in a periodic flow domain with a pseudo-spectral code. In spectral space, the Navier-Stokes equations read

$$\left(\frac{\partial}{\partial t} + \nu|\boldsymbol{k}|^2\right) u_\alpha(\boldsymbol{k},t) = M_{\alpha\beta\gamma}(\boldsymbol{k}) \sum_{\boldsymbol{p}+\boldsymbol{q}=\boldsymbol{k}} u_\beta(\boldsymbol{p},t) u_\gamma(\boldsymbol{q},t) + F_\alpha(\boldsymbol{k},t), \tag{1}$$

with $M_{\alpha\beta\gamma}(\boldsymbol{k}) = \frac{1}{2i}\Big(k_\beta D_{\alpha\gamma}(\boldsymbol{k}) + k_\gamma D_{\alpha\beta}(\boldsymbol{k})\Big)$ and $D_{\alpha\beta}(\boldsymbol{k}) = \delta_{\alpha\beta} - k_\alpha k_\beta/|\boldsymbol{k}|^2$. Here, ν is the kinematic viscosity, $u_\alpha(\boldsymbol{k},t)$ is the Fourier coefficient of the velocity field at wave vector $\boldsymbol{k}$ and time t, and F_α is the time-modulated forcing.

First, we recall that traditional agitation of the large-scale structures in a turbulent flow may be achieved by introducing a forcing term restricted to wave vectors with $|\boldsymbol{k}| \le k_F$, *i.e.*, identifying a forcing range through the upper-limit k_F. Specifically, we force the turbulence similarly as in [7, 11],

$$f_\alpha(\boldsymbol{k},t) = \frac{\varepsilon_w}{N_F} \frac{u_\alpha(\boldsymbol{k},t)}{|\boldsymbol{u}(\boldsymbol{k},t)|^2}, \qquad |\boldsymbol{k}| \le k_F, \tag{2}$$

where ε_w is the constant energy injection rate and $N_F = N_F(k_F)$ is the total number of forced modes. For convenience, the wave vectors are grouped in spherical shells with the n-th shell containing all modes such that $\frac{2\pi}{L_b}(n-1/2) < |\boldsymbol{k}| \le \frac{2\pi}{L_b}(n+1/2)$, where L_b is the box-size in physical space. We apply large-scale forcing either in the first shell (*i.e.*, $k_F = 3\pi/L_b$ which implies $N_F = 18$, the case considered in [2]) or in the first two shells (*i.e.*, $k_F = 5\pi/L_b$ which

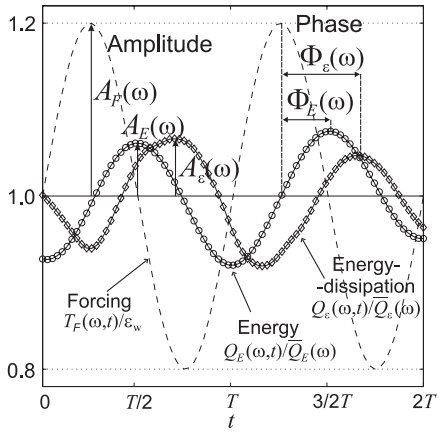

Fig. 1 – The amplitudes $A_F(\omega)$, $A_E(\omega)$, $A_\varepsilon(\omega)$ and phase-shifts $\Phi_F(\omega) \equiv 0$, $\Phi_E(\omega)$, $\Phi_\varepsilon(\omega)$ of the forcing $T_F(\omega,t)$ (dashed line), the energy $Q_E(\omega,t)$ (labeled $\circ$), and the energy dissipation rate $Q_\varepsilon(\omega,t)$ (labeled $\diamond$) normalized by their respective means $\overline{T}_F = \varepsilon_w$, $\overline{Q}_E(\omega)$, and $\overline{Q}_\varepsilon(\omega)$ obtained from simulations at the modulation frequency $\omega = 0.8\pi$.

implies $N_F = 80$). The second step in specifying the forcing F_α introduces the periodic time modulation

$$F_\alpha(\boldsymbol{k},t) = f_\alpha(\boldsymbol{k},t)\Big(1 + A_F \sin(\omega t)\Big), \tag{3}$$

where A_F is the amplitude of modulation and ω its angular frequency. The modulated forcing corresponds to a total energy input rate which oscillates around ε_w with amplitude A_F,

$$T_F(\omega,t) = \sum_{\boldsymbol{k}} u^*_\alpha(\boldsymbol{k},t) F_\alpha(\boldsymbol{k},t) = \varepsilon_w\Big(1 + A_F \sin(\omega t)\Big). \tag{4}$$

The length and time scales of the numerical simulation are chosen by picking $L_b = 1$ for the box size in physical space, and $\varepsilon_w = 0.15$ for the energy injection rate. The Reynolds number is then determined by the dimensionless viscosity ν. Choosing $\nu^{-1} = 1060.7$ and $\nu^{-1} = 4242.6$ results in respective Taylor-Reynolds numbers $R_\lambda \cong 50$ and $R_\lambda \cong 100$. We use these two cases as references denoted by R_{50} and R_{100}. The spatial resolution needed may be estimated by requiring $k_{\max}\eta > 1$ with η the Kolmogorov dissipation scale and $k_{\max}$ the highest wave number included in the spatial discretization. For the R_{50} case a resolution of at least 64^3 computational points is required, while for R_{100} a higher resolution of 192^3 points is necessary. The latter poses a strong computational challenge in view of the extensive ensemble averaging and large number of modulation frequencies. However, it was found that many large-scale quantities, such as the total energy, do not depend too sensitively on resolution.

Averaging procedure and simulation setting. – In order to analyze the response to a time-modulated forcing, the precise extraction of the amplitude and phase of the conditionally averaged variations is a key issue. Two steps can be distinguished, *i.e.*, the computation of the conditionally averaged signal itself and the subsequent determination of amplitude and phase characteristics of this signal, see fig. 1.

We adopt ensemble averaging to determine the conditionally averaged signal $S(\omega,t)$, where $S(\omega,t)$ is the total energy $E(\omega,t)$, the Taylor-Reynolds number $R_\lambda(\omega,t)$, or the energy dissipation rate $\varepsilon(\omega,t)$. Ensemble averaging requires a sufficiently large sample of statistically independent signals $\{S_j(\omega,t)\}$ to be generated. We compute the unmodulated flow and store

N_r realizations of the turbulent solution corresponding to $t > 10$. The latter condition allows transients related to the initial condition to become negligible. The time separation between these snapshots is larger than two eddy turnover times. Subsequently, each of these N_r realizations was taken as the initial condition for a simulation with time-modulated forcing at a particular frequency ω. This provides N_r sample signals which need to be averaged to obtain the conditionally averaged signal $S(\omega, t)$. Repeating this procedure for a range of frequencies yields the total response characteristics. Given the conditionally averaged response signal $S(\omega, t)$, there are various ways in which amplitude and phase information can be extracted. In [8] the signal $S(\omega, t)$ is first averaged over time to yield $\overline{S}(\omega)$. Subsequently, the normalized variation defined as $Q_S^{(a)}(\omega, t) = S(\omega, t)/\overline{S}(\omega)$ is studied using the Fourier transform ($\mathcal{F}$) in which time t is transformed into frequency f. Correspondingly, the power amplitude spectrum $\widehat{Q}_S^{(a)}(\omega, f) = \mathcal{F}\big(Q_S^{(a)}(\omega, t) - 1\big)$ can be obtained, which assumes a maximum value $A_S(\omega) = \max\{|\widehat{Q}_S^{(a)}(\omega, f)|\}|_{f=f_A(\omega)}$, as denoted in fig. 1 for forcing $A_F(\omega)$, total energy $A_E(\omega)$, and energy dissipation rate $A_\varepsilon(\omega)$. The maximum $A_S(\omega)$ as the amplitude at dominant frequency can be used to quantify the response as a function of the modulation frequency ω. This approach is accurate if the Fourier transformation is applied to an integer number of modulation periods. The method used in [2] is based on a fitting procedure in which it is assumed that $S(\omega, t) \approx \overline{S} + A_S \sin\big(\omega t + \Phi_S\big)$. The dependence of the parameters $\{\overline{S}, A_S, \Phi_S\}$ on ω may be obtained from a least-squares procedure. This evaluation method assumes that the conditionally averaged signal has the same frequency as the forcing.

At modest ensemble size N_r it is beneficial to explicitly incorporate variations in the unmodulated reference signal to improve the data evaluation. This motivates an alternative method in which we determine N_r sample signals $\{S_j(\omega, t)\}$ corresponding to the modulated case, as well as N_r unmodulated signals $\{s_j(t)\}$ that start from the same set of initial conditions. This allows to generate different "normalized" signals such as $Q_S^{(b)}(\omega, t) = \sum_j S_j / \sum_j s_j$ or $Q_S^{(c)}(\omega, t) = \sum_j S_j/s_j/N_r$. These normalized signals provide estimates that compensate to some degree for the relatively small number of samples or for an unknown mean component but have the drawback that they cannot be applied in the context of a physical experiment. Additionally, we divided these signals by its means (time averages) and removed the constant component corresponding to the zero-frequency response. Application of the Fourier transform, $\widehat{Q}_S^{(b)} = \mathcal{F}\big(Q_S^{(b)}/\overline{Q}_S^{(b)} - 1\big)$ and $\widehat{Q}_S^{(c)} = \mathcal{F}\big(Q_S^{(c)}/\overline{Q}_S^{(c)} - 1\big)$, provides direct access to amplitude and phase information. Each of these methods yields the same general impression of response maxima in time-modulated turbulence. Differences arise only on a more detailed level of the processed data but these do not obscure the interpretation of the main features of the response. Therefore we only present results extracted from the normalized signal $Q_S/\overline{Q}_S \equiv Q_S^{(c)}/\overline{Q}_S^{(c)}$, unless explicitly stated otherwise. The simulations were performed in the frequency range $\pi/5 \leq \omega \leq 80\pi$ with time-modulated forcing at an amplitude $A_F = 1/5$. For each of the N_r unmodulated initial conditions, $n_T = 4$ periods of the modulated forcing were simulated, *i.e.*, each sample signal was computed for $n_T T$ time units with modulation period $T = 2\pi/\omega$. Since an explicit time-stepping method was adopted, the cases at low ω add particularly to the total computational cost. The number of realizations required in the ensemble was investigated separately. Results for several modulation frequencies were compared at $N_r = 10$, 30 and 50; it was found that 30 independent samples provide adequate statistical convergence for our purposes. We stored $N_t = 40$ points per modulation period and present results obtained by evaluating the last two recorded periods, *i.e.*, $2T \leq t \leq 4T$. Comparison with results obtained by evaluating data on $0 \leq t \leq 4T$ yielded only minor differences. Finally, the phase $\Phi_S(\omega)$ between the forcing

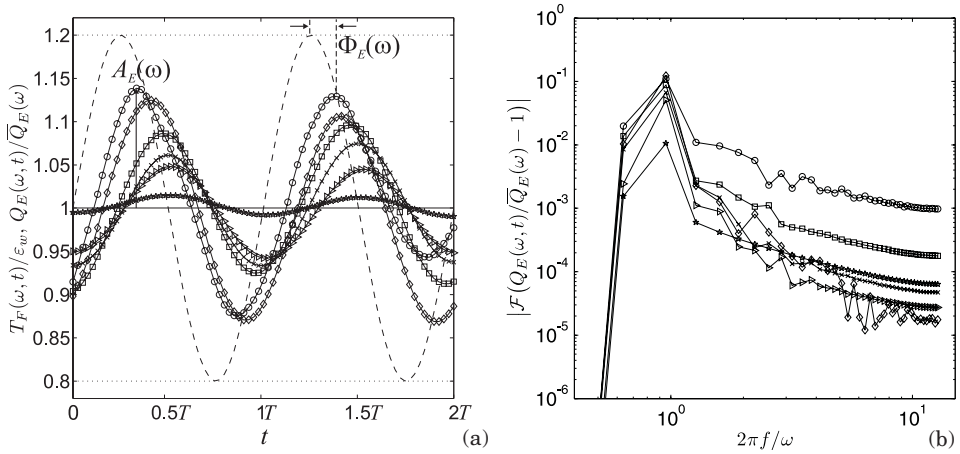

Fig. 2 – The response $Q_E(\omega,t)/\overline{Q}_E(\omega)$ for the R_{50} case recorded at different modulation frequencies ω is shown in (a) together with the modulation of the forcing $T_F(\omega,t)/\varepsilon_w$ (dashed line). The corresponding power spectra of the Fourier transform as a function of the transformed frequency f are collected in (b). Modulation frequencies $\omega/(2\pi) = 0.1,\ 0.2,\ 0.3,\ 0.4,\ 0.5,\ 2.0$ are included and labeled by $\circ$, $\diamond$, $\square$, $\times$, $\triangleright$ and $\star$, respectively.

and the response can be computed from the Fourier-transformed data as well. At the dominant frequency f_A of the transformed signal $\widehat{Q}_S(\omega,f) = \mathcal{F}\big(Q_S(\omega,t)\big)/\overline{Q}_S(\omega,t) - 1\big)$, the phase becomes $\Phi_S(\omega) = \arctan\big(\mathrm{Im}(\widehat{Q}_S(\omega,f_A))/\mathrm{Re}(\widehat{Q}_S(\omega,f_A))\big)$.

Modulated turbulence. – In fig. 2(a) the conditionally averaged signal $Q_E(\omega,t)/\overline{Q}_E(\omega)$ based on total energy is shown at a number of modulation frequencies. The conditionally averaged response has a clear oscillatory behavior. The Fourier transform of the data from fig. 2(a) is shown in fig. 2(b) and displays a dominant maximum corresponding to the forcing frequency $f_A = \omega/(2\pi)$. This observation confirms that the least-squares–fitting procedure adopted in [2] is justified.

We now focus on the amplitude of the total energy response as a function of the modulation frequency ω. The amplitude $A_E(\omega)$ computed as maximum of the Fourier-transformed normalized signal for each modulation frequency is shown in fig. 3(a). The maximum response appears at $\omega_{\max} \approx 1.5$, in accordance with the expectation [1, 2] that it should be close to the inverse large eddy turnover time. In addition, the location of the maximum is not very sensitive to R_λ, reflecting that the response maximum is mainly associated with the large-scale features in the flow. At high modulation frequencies, $\omega > \omega_{\max}$, the decay of A_E is proportional to ω^{-1}, which becomes particularly visible in the compensated response $\omega A_E(\omega)$, fig. 3(b). At very low modulation frequencies, $\omega < \omega_{\max}$, a plateau in $A_E(\omega)$ must of course develop [1, 2], as the turbulence then completely follows the forcing. Our simulations do not achieve small enough ω to observe a pronounced plateau. The maximum of $\omega A_E(\omega)$ is about 35% higher as compared to the value at high ω. This is as expected lower than predicted by the mean-field theory described in [1] as the fluctuations slightly smear out the mean-field maximum, but it is much more pronounced compared to results based on the GOY or REWA simulations [2]. The reason is that, although the appearance of the response maxima is a large-scale effect, the correct resolution of the small-scales is important for a proper quantitative representation of the effect, because the small-scale resolution affects the energy flux downscale. We also calculated the response curves for the Taylor-Reynolds number; the results are quite similar.

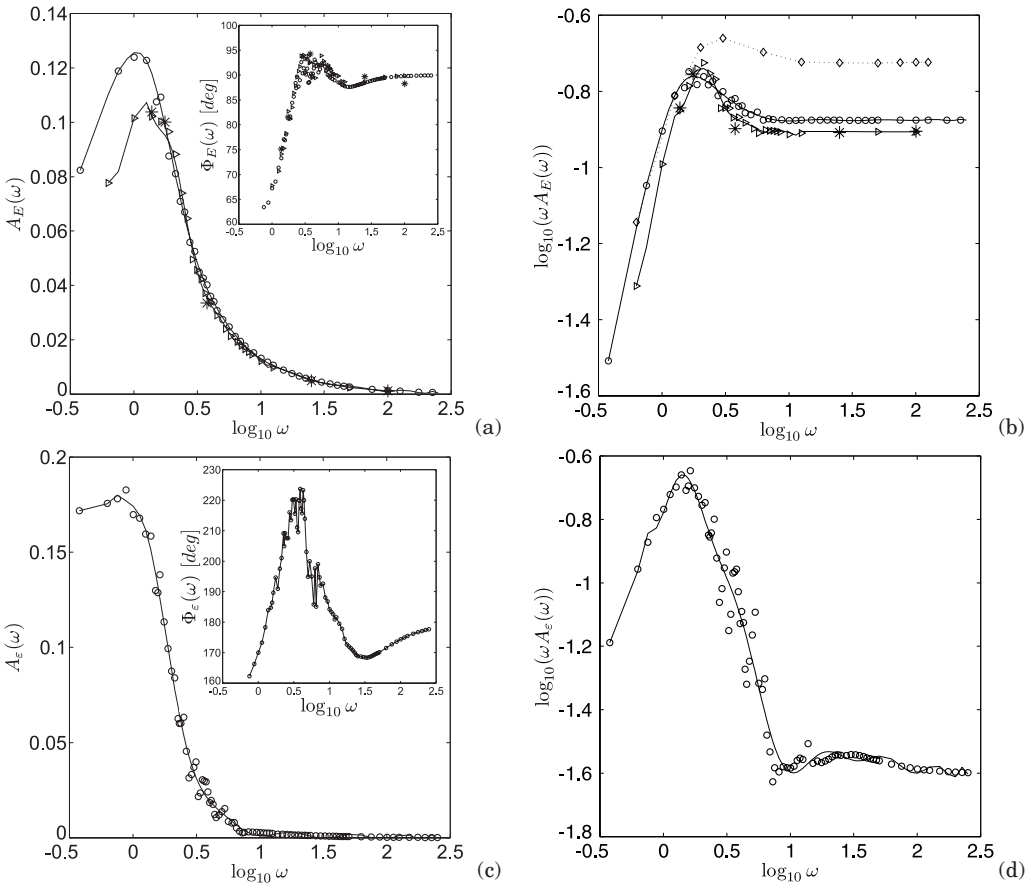

Fig. 3 – Amplitudes $A_E(\omega)$ (a), $A_\varepsilon(\omega)$ (c) and compensated amplitudes $\omega A_E(\omega)$ (b), $\omega A_\varepsilon(\omega)$ (d) for the energy and energy dissipation rate obtained for R_{50} (labeled $\circ$) and R_{100} (labeled $\triangleright$) cases. Verification at selected frequencies for resolution 128^3 and R_{100} case (labeled $\star$). Results for R_{50} case forced in two first shells (labeled $\diamond$). The insets show the phase-shift between the energy $\Phi_E(\omega)$ (a) and energy dissipation rate responses $\Phi_\varepsilon(\omega)$ (b), and the forcing modulation.

The phase difference between the forcing modulation and the conditionally averaged total energy response is shown in fig. 3(a) as inset. We observe a strong variation in this phase difference for modulation frequencies near the most responsive modulation frequency. It appears that the maximum response as shown in fig. 3(a)-(b) occurs at a modulation frequency where also the variation in the phase difference is largest. Very recently, a strong phase shift was also found in windtunnel experiments in which a time modulation is introduced via a periodic cycling of an upstream active grid. In these experiments the maximum response was found to shift to higher frequencies in case the characteristic length scales of the forcing were reduced [12]. Can such a dependence on the type of forcing also be observed in our numerical simulations? To find out we force a higher wave number band of modes ($k_F \leq 5\pi/L_b$) instead of restricting us entirely to low wave number forcing. The result is seen in fig. 3(b) indicated by $\diamond$. Indeed, for this type of forcing the response maximum is seen to shift to higher ω and becomes less pronounced. Further quantitative connections with physical experiments such as the influence of anisotropy [10] are currently being investigated.

The energy dissipation rate in the system is a quantity that is accessible to direct physical experimentation. In fig. 3(c)-(d) we show the energy dissipation rate amplitudes $A_\varepsilon(\omega)$, $\omega A_\varepsilon(\omega)$. We notice that at high modulation frequency ω the amplitude approaches zero, consistent with the expectation that the modulation of the forcing is not effective in this range. More importantly, the energy dissipation rate amplitude displays a strong response maximum at the level of 85% compared to the amplitude of modulation. The total mean energy dissipation $T^{-1}\int_0^T \varepsilon(\omega, t)\mathrm{d}t$ for each modulation frequency ω is almost constant. It differs from the energy input rate $\varepsilon_w = 0.15$ at the level of 1% for most of the frequencies, reaching the maximum difference of 5% for the lowest simulated frequency, confirming good numerical convergence. This is in agreement with boundary layer experiments [10] where the *time-averaged* quantities are only slightly affected by the imposed oscillations.

Summary. – The direct numerical simulation of the response of turbulence to time-modulated forcing confirms the existence of a response maximum. The simulation findings are in general agreement with predictions based on a mean-field theory [1]. The mean-field theory predicts the decrease of the response amplitude proportional to ω^{-1} as the modulation frequency is sufficiently large which was observed in the simulations as well. The response maxima in the total energy and the Taylor-Reynolds number occur at the forcing frequencies of the order of the inverse large eddy turnover time scale. The phase-difference between the modulation of the forcing and the conditionally averaged response displays a strong dependence on the modulation frequency as well. The modulation frequency at which the response maximum arises depends only weakly on the Reynolds number but shows a dependence on the scales included in the forcing as well as on the flow property that is considered. In general, if the particular quantity of interest shows a stronger dependence on the smaller scales in a turbulent flow, then the response maximum arises at a somewhat higher frequency. These findings may be independently assessed in physical experiments, *e.g.*, conducted in wind tunnels combined with the use of active grids cycled in a periodic sequence [12].

* * *

Stimulating discussions with W. van der Water (Eindhoven University of Technology) are gratefully acknowledged. This work is sponsored by the Foundation for Fundamental Research on Matter (FOM). The authors wish to thank SARA Computing and Networking Services for providing the computational resources.

REFERENCES

[1] von der Heydt A., Grossmann S. and Lohse D., *Phys. Rev. E*, **67** (2003) 046308.
[2] von der Heydt A., Grossmann S. and Lohse D., *Phys. Rev. E*, **68** (2003) 066302.
[3] Biferale L., *Annu. Rev. Fluid Dyn.*, **35** (2003) 441.
[4] Bohr T., Jensen M. H., Paladin G. and Vulpiani A., *Dynamical Systems Approach to Turbulence* (Cambridge University Press, Cambridge) 1998.
[5] Kadanoff L., Lohse D., Wang J. and Benzi R., *Phys. Fluids*, **7** (1995) 617.
[6] Eggers J. and Grossmann S., *Phys. Fluids A*, **3** (1991) 1958.
[7] Grossmann S. and Lohse D., *Z. Phys. B*, **89** (1992) 11; *Phys. Rev. E*, **50** (1994) 2784.
[8] Cadot O., Titon J. H. and Bonn D., *J. Fluid Mech.*, **485** (2003) 161.
[9] Camussi R., Ciliberto S. and Baudet C., *Phys. Rev. E*, **56** (1997) 6181; Caponeri M. and Ciliberto S., *Physica D*, **58** (1992) 365.
[10] Tardu S. F., Binder G. and Blackwelder R. F., *J. Fluid Mech.*, **267** (1994) 109.
[11] Ghosal S., Lund T. S., Moin P. and Akselvoll K., *J. Fluid Mech.*, **286** (1995) 229.
[12] Tipton C. and van der Water W., submitted to *Phys. Rev. Lett.*, 2005.